ELSEVIER

Applied Acoustics 63 (2002) 595–609

applied acoustics

www.elsevier.com/locate/apacoust

Sound propagation around rigid barriers laterally confined by tall buildings

Luís Godinho, Julieta António, António Tadeu*

Department of Civil Engineering, University of Coimbra, Polo II - Pinhal de Marrocos, 3030 Coimbra, Portugal

Received 8 May 2001; received in revised form 2 October 2001; accepted 9 October 2001

Abstract

This paper focuses on the propagation of sound waves in the presence of acoustic barriers placed close to very tall buildings. The boundary element method (BEM) is used to model the acoustic barrier, while the presence of the tall buildings is taken into account by using the image source method. Different geometries are analyzed, representing the cases of a single building, two buildings forming a corner and three buildings defining a laterally confined space. The acoustic barrier is assumed to be non-absorbing, and all the buildings and the ground are modeled as infinite rigid plane surfaces. Calculations are performed in the frequency domain and time signals are then obtained by means of Inverse Fourier Transforms. The sound pressure loss provided by the acoustic barrier is computed, illustrating the importance of the lateral confinements.

1. Introduction

Empirical methods are often used by engineers to face some practical problems, like the use of acoustic barriers to deaden the traffic noise. However, it would be useful to know more about sound propagation close to such barriers, and considerable research has been done to develop numerical methods for studying the problem.

Various approaches have been tried, such as diffraction-based methods and other simplified schemes [1,2], to calculate the energy loss due to the presence of an acoustic barrier.

More accurate results can be obtained by making use of the BEM or the finite element method. However, these methods are extremely costly in terms of computer

* Corresponding author. Tel.: +351-239-797-204; fax: +351-239-797-190.
E-mail address: meccc@dec.uc.pt (A. Tadeu).

0003-682X/02/$ - see front matter
PII: S0003-682X(01)00064-0

effort, making their application to very high frequencies difficult. Duhamel [3] described a numerical method that was based on the boundary element method, employing a set of 2D solutions to calculate the 3D sound pressure around an acoustic barrier that has a constant, but arbitrary cross-section. Duhamel and Sergent [4] further developed this work so that absorption by the ground could be taken into consideration, which also made it possible to compare the numerical and experimental results. A 2D boundary element model was used by Morgan et al. [5] to evaluate the importance of the shape and surface-absorption of barriers built to deaden rail traffic noise. Lacerda et al. [6] developed a dual boundary element method to study the propagation of two-dimensional sound around acoustic barriers over an infinite plane, where the ground and the barrier were both absorptive. Later, Lacerda et al. [7] used a dual boundary element formulation to analyze the propagation of three-dimensional sound around an absorptive barrier, modeling the barrier as a simple surface. This method avoided the problems caused by near-singular integrals and near-degenerate equation systems. These authors employed a Green's function that considered the properties of the ground, which made it possible to model absorptive ground. Jean et al. [8] have studied the effectiveness of noise barriers at deadening road traffic noise, using a 2D boundary element method, and modeling point sources, coherent and incoherent line sources. Their 3D responses were arrived at by a post-treatment of the 2D findings, and their model assumed that the acoustic barrier and the ground surface were absorptive.

The authors have recently published work on the evaluation of the acoustic scattering of a three-dimensional sound source by an infinitely long rigid barrier in the vicinity of tall buildings using the BEM [9]. The barrier was assumed to be non-absorbing and the building was modeled as an infinite barrier. The presence of the building was taken into account by defining the required BEM Green's function using the image method. Thus, only the boundaries of the barrier needed to be discretized. Different geometric models, with barriers of varying sizes, were used. The reduction of sound pressure in the vicinity of the buildings was evaluated and the creation of shadow zones by the barriers was analyzed and compared with results provided by a simplified method. However, in that work, the barrier was assumed to be infinitely long.

The geometry of the acoustic barrier was assumed to be constant in one direction (z). Such a situation is frequently referred to as a two-and-a-half-dimensional problem (or 2-1/2-D), for which solutions can be obtained by means of a spatial Fourier transform in the direction in which the geometry does not vary. This requires solving a sequence of 2D problems with different spatial wavenumbers k_z [10,11]. Then the inverse Fourier transform is used to synthesize the 3D field.

This paper expands the earlier work. It handles the problem of pressure wave scattering, generated by a point load in the vicinity of an acoustic barrier, which is here considered to be bounded by one or two lateral walls. These are simulated by means of the image source technique, which places virtual sources along the longitudinal direction of the barrier. The model thus created tries to represent the cases of a sound barrier when confined by lateral buildings, forming an L or U configuration, more realistically. This type of geometry may be found in complex urban

environments where a specific building façade, confined by lateral buildings, needs to be protected from exterior noise sources.

This paper is divided into three parts. First there is a description of the 3D acoustic BEM formulation in the frequency domain. The Green's functions required for modeling the different geometries are presented. Then, the calculation of the time domain response is briefly described. Finally, the model is used to compute the three-dimensional pressure field generated by a point pressure source in the vicinity of the buildings, for the different scenarios defined. Time responses and sound attenuation are given for different-sized barriers.

2. Problem definition

This work computes the pressure field around an acoustic barrier in the vicinity of a tall building placed parallel to the barrier. The geometry of the barrier is assumed to be constant in one direction (z axis). The solution is obtained in two steps. First, the solution is calculated for a barrier of infinite length. Next, the presence of lateral vertical walls is simulated, using virtual sources placed along the longitudinal direction.

BEM is used to obtain the solution for the first step. The full details of the formulation required are not given here, since this problem has already been solved by the authors [10,11]. It is sufficient to state that the 3D solution is obtained by adding together the 2D BEM solutions for the different spatial wavenumbers given when a spatial Fourier transformation is applied along the z axis. Each problem is solved for $k_\alpha = \sqrt{\frac{\omega^2}{\alpha^2} - k_z^2}$, where α is the pressure wave velocity, ω is the excitation frequency and k_z is the axial wavenumber. If we take an infinite set of sources, placed along the z direction at equal intervals, L, to allow the axial wavenumber to be defined as $k_{zm} = \frac{2\pi}{L}m$, the full three-dimensional solution is synthesized as a discrete summation,

$$p(\omega, x, y, z) = \frac{2\pi}{L} \sum_{m=-\infty}^{\infty} \hat{p}(\omega, x, y, k_{zm}) \mathrm{e}^{-ik_{zm}z} \tag{1}$$

in which $i = \sqrt{-1}$. This equation behaves well and can be approximated by a finite sum of terms ($m = -M, M$).

This model avoids the 3D discretization of the surface of the barrier, requiring only the 2D cross-section to be discretized. Each BEM model requires the evaluation of the integral

$$H^{kl} = \int_{C_l} H\left(\underline{x}_k, \underline{x}_l, n_l\right) dC_l \tag{2}$$

in which H^{kl} is the pressure velocity component at $\underline{x}_k$ caused by the pressure load at $\underline{x}_l$ and n_l is the unit outward normal for the lth boundary segment C_l. The pressure velocity is obtained by differentiating the corresponding Green's function.

For a harmonic line pressure load placed inside an infinite fluid medium at position (x_0, y_0), the Green's function is given by

$$G(x, x_0, y, y_0, k_\alpha) = -\frac{i}{4} H_0(k_\alpha r) \tag{3}$$

where H_0 is the Hankel function of the second type and order 0.

The pressure field defined by Eq. (3) must be reformulated to satisfy the boundary conditions at the rigid ground and building wall, which require null normal velocities. These conditions can be satisfied automatically by superposing the pressure field generated by the real source [placed at (x_0, y_0)] plus three virtual sources (image sources), located in such a way that they constitute mirrors in relation to the vertical and horizontal planes. This mirror technique can be visualized as a superposition of the actual source and sound fields reflected from the ground and the walls of the buildings. Thus, only the cross-section of the barrier needs to be discretized. Note that this technique is applicable since the ground and the building façades are assumed to be flat and rigid. The pressure field [Green's function $G(x,x_0,y,y_0,k_\alpha)$] can then be computed by the following expression, when the vertical plane and the horizontal plane are defined by $x=0$ and $y=0$, respectively:

$$G(x, x_0, y, y_0, k_\alpha) = \sum_{j=1}^{NS} \frac{-i}{4} \left[H_0\left(k_\alpha r_j\right) \right] \tag{4}$$

in which $NS=4$,

$$r_1 = \sqrt{(x - x_0)^2 + (y - y_0)^2}$$
$$r_2 = \sqrt{(x - x_0)^2 + (y + y_0)^2}$$
$$r_3 = \sqrt{(x + x_0)^2 + (y - y_0)^2}$$
$$r_4 = \sqrt{(x + x_0)^2 + (y + y_0)^2}$$

To simulate the presence of either one or two lateral, vertical, flat surfaces, one needs to assume the existence of additional virtual point sources, placed along the longitudinal direction. Again, the mirror technique is used, and these virtual sources are positioned so that they satisfy the boundary conditions of the lateral walls. When only one vertical wall is placed at $z=50.0$ m and the real source is at (x_0, y_0, z_0), the solution uses a single virtual source, leading to the incident pressure field,

$$p(x, y, z, \omega) = \frac{2\pi}{L} \sum_{m=-M}^{M} \hat{p}(x, y, k_{zm}, \omega) \left(e^{-ik_{zm}(z - z_0)} + \mathrm{e}^{-ik_{zm}(100.0 - z - z_0)} \right) \tag{5}$$

When the acoustic system is confined by two vertical lateral walls, the solution is computed using an infinite number of virtual sources, as defined in the following equation,

$$p(x, y, z, \omega) = \frac{2\pi}{L} \sum_{m=-M}^{M} \left[\hat{p}(x, y, k_{zm}, \omega) \left(e^{-ik_{zm}(z-z_0)} + \sum_{n=1}^{NSZ} \sum_{i=1}^{4} \mathrm{e}^{-ik_{zm}z_i} \right) \right] \tag{6}$$

where

$$z_1 = |z + z_0 + 2an|$$
$$z_2 = |z - 2a - z_0 - 2an|$$
$$z_3 = |z + 2a - z_0 + 2an|$$
$$z_4 = |z - 2a + z_0 - 2an|$$

a is the distance between lateral walls.

The number of sources (NSZ) allows the signals to be fully defined within the time interval fixed by the frequency increment.

3. Pressure in time-space

The pressures in the time domain can be obtained by fast Fourier transforming in ω the synthesized 3D field, assuming the source to have a temporal variation defined by a Ricker pulse. The rapid decay of this pulse, in both the time and frequency domains, allows computational effort to be reduced and the results obtained in the time domain can be more easily interpreted.

The Ricker function can be expressed by:

$$u(\tau) = A\left(1 - 2\tau^2\right)e^{-\tau^2} \tag{7}$$

in which A is the amplitude, $\tau = (t - t_s)/t_0$ and t represents the time, with t_s being the time when the maximum occurs, while πt_0 is the dominant wavelet period. By applying a Fourier transformation to this function, one obtains:

$$U(\omega) = A\left[2\sqrt{\pi t_0}e^{-i\omega t_s}\right]\Omega^2 e^{-\Omega^2} \tag{8}$$

where $\Omega = \omega t_0/2$.

Complex frequencies with an imaginary part of the form $\omega_c = \omega - i\eta$ (with $\eta = 0.7\Delta\omega$) are used to reduce the influence of the virtual sources placed along the longitudinal direction and to avoid the aliasing phenomena. The response in the time domain is subsequently rescaled, applying an exponential window $e^{\eta t}$ [12].

4. Numerical examples

All the examples presented here refer to an acoustic barrier of height h, placed in front of a tall building, with its inner face 20.0 m away from it, to reduce the sound

level registered on its façade (see Fig. 1). In the first example, the acoustic barrier is considered to have an infinite length (Fig. 1a). The second situation, assumes the presence of a lateral, vertical, flat surface, bounding one side of the acoustic barrier (Fig. 1b). The third example is the case of an acoustic barrier limited by vertical surfaces on both sides (Fig. 1c) 50.0 m away from each other.

At time $t = 0.0$ s, the acoustic medium is struck by a pressure source, placed either at $z = 25.0$ m (source 1), or at $z = 45.0$ m (source 2). In both cases, the source is considered to be 0.6 m above the ground and 25.0 m from the tall building. Notice that, when two lateral walls are modeled, the source 1 is on the plane of symmetry. Each source creates a spherical pressure pulse that propagates away from its origin. The pressure wave propagation velocity of 340.0 m/s is kept constant for all the analyses. Computations are performed for acoustic barriers of different heights ($h = 0.0$, 2.0 and 6.0 m). The pressure field generated by each source is evaluated at a grid of receivers placed along a vertical plane 0.5 m away from the rigid longitudinal wall (i.e. $x = 0.5$ m), and equally spaced at intervals of 1.0 m vertically, and 0.5 m longitudinally.

The calculations are performed in the 2.5–320.0 Hz frequency range, with 2.5 Hz increments. The source time dependence is assumed to be a Ricker wavelet with a characteristic frequency of 125 Hz. The frequency increment permits the dynamic analysis of the event for 0.4 s, a value that is not sufficient for the total development of the response. To permit analysis of the signal in time, a complex part was introduced into each excitation frequency to ensure damping of the response at the end of the time window, which was taken as ($1/\Delta f = 0.4$ s), as described above.

In this work, the acoustic barrier is assumed to be a body 0.2 m thick. The surface of the barrier is discretized using a number of boundary elements defined by setting

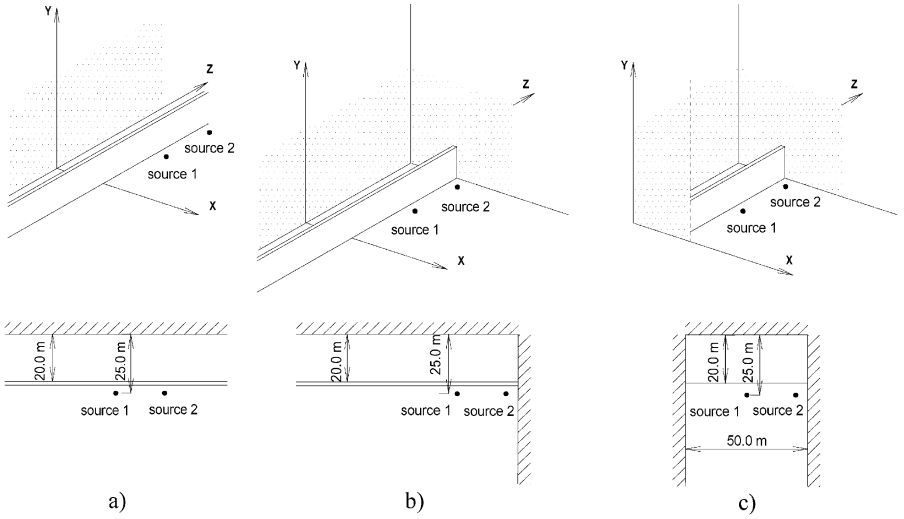

Fig. 1. Schematic representation of the different scenarios: (a) laterally unbounded system; (b) acoustic system confined by one lateral wall; (c) acoustic system confined by two lateral walls.

to 8 the relation between the wavelength and the length of boundary elements. In no case are fewer than 32 elements used. In order to maintain accuracy, the numerical integrations [Eq. (6)] required for the BEM are achieved by making use of a Gauss–Legendre quadrature integration scheme. The number of sampling points for this scheme increases as the distance between the loaded element and the element to be integrated decreases.

In the first part of this section, the time domain responses calculated for the different geometric configurations are presented and discussed, to better understand the sound propagation phenomenon. After this analysis, a brief description of the procedure used to obtain the sound pressure level (SPL) attenuation is presented, and applied to one of the cases studied. Finally, the last part of this section presents the SPL attenuation for the scenarios described earlier.

4.1. Time responses generated by source 1

To better illustrate the propagation of the sound pressure from its source to the receivers, the time responses are presented as a sequence of snapshots. At time $t = 0.0$ ms a spherical pulse is emitted from a point pressure source, located at $x = 25.0$ m, $y = 0.6$ m and $z = 25.0$ m (source 1).

Fig. 2 displays the pressure wave field responses obtained at $t = 90.6$ ms, $t = 120.3$ ms and $t = 240.3$ ms for the three different scenarios. In these plots, the pressure amplitude is represented by a gray scale ranging from white to black, as the amplitude increases.

As the pulse propagates away from the source, the wave energy spreads out. At time $t = 90.6$ ms the incident pulse has already hit the grid of receivers (see Fig. 2; $t = 90.6$ ms). When the barrier is absent, the response recorded at the receivers is stronger, while it suffers a pronounced decay as the size of the barrier increases, particularly for receivers placed lower down. However, the interaction of the direct pulses, diffracted from the edge of the barrier, with those first reflected by the ground, produces an enhanced response at the receivers placed in the close vicinity of the ground. This pulse reflected on the ground is even clearly visible as a second pulse when the barrier is present. When a barrier 6.0 m tall is inserted between the source and the receivers, the wave-front development is smaller. This is because the larger size of the barrier means that the waves from the source need to travel a longer path before hitting the receiver. Notice that, at this time ($t = 90.6$ ms), the presence of the lateral walls does not influence the response, because the incident and the scattering pulses hitting these surfaces have not yet reached the receivers.

As time progresses, the pulse travels further away from the source. For $t = 120.3$ ms, in the absence of any lateral wall (Fig. 2a; $t = 120.3$ ms), the wavefront becomes larger, but the response maintains the same features as explained above. When a barrier is inserted between the source and the receivers, as explained before, two different pulses are originated. However, as the time advances they draw further apart and become easier to identify (see Fig. 2; $t = 90.6$ ms and $t = 120.3$ ms). When the lateral walls are present, the complexity of the scattered field increases, as they originate additional wave reflections. If only one lateral wall is modeled, the first

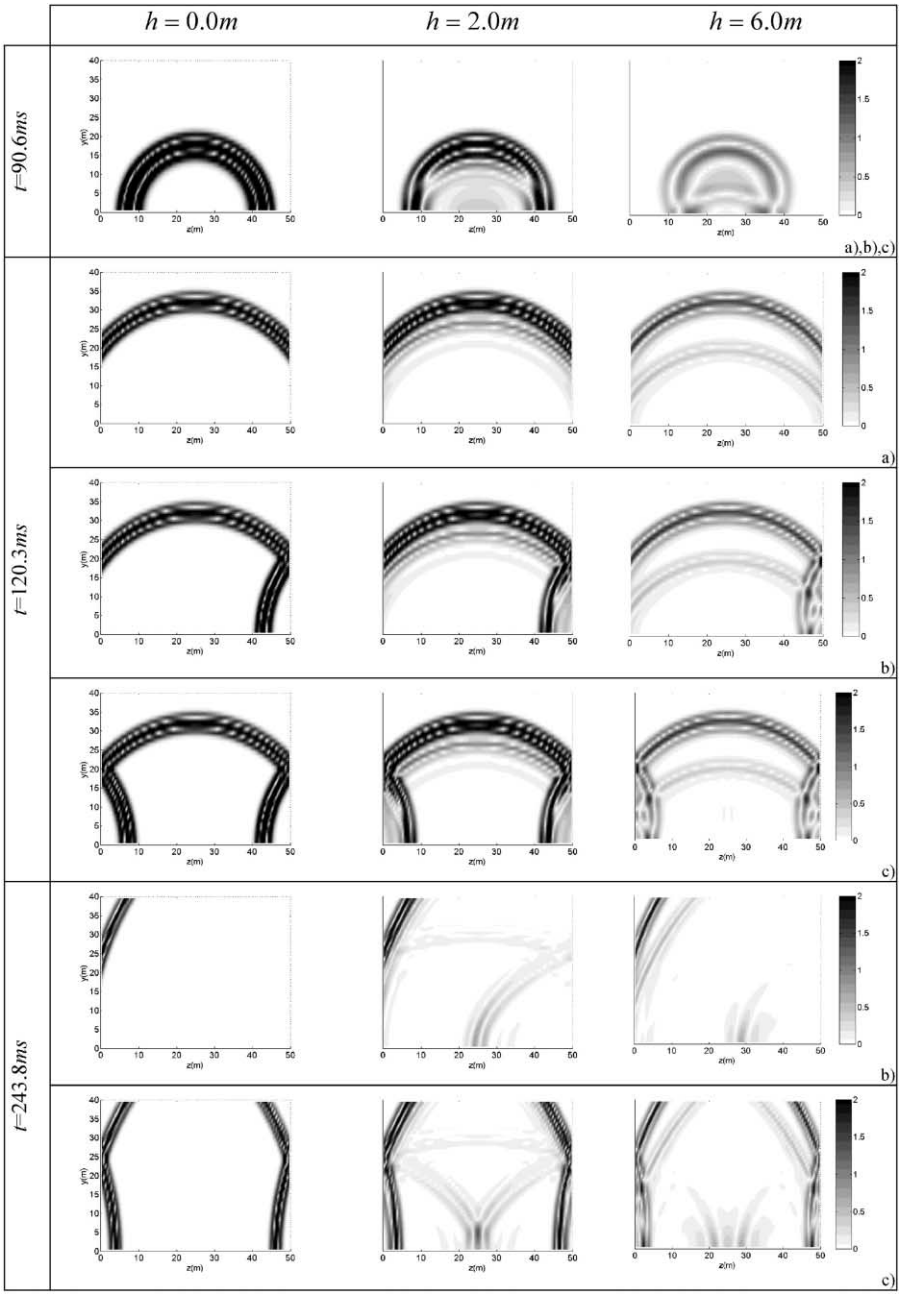

Fig. 2. Time domain responses for the different scenarios: (a) no lateral confinements; (b) one lateral wall at $z = 50.0$ m; (c) two lateral walls at $z = 0.0$ m and $z = 50.0$ m.

reflected pulses on this surface become clearly distinguishable as a set of pulses travelling from right to left (see Fig. 2b; $t = 120.3$ ms). Similar behavior is registered when the propagation domain is confined on both sides, originating a second set of reflected pulses travelling from left to right (see Fig. 2c; $t = 120.3$ ms). As before, the pulses resulting from reflections on the ground, after being diffracted from the edge of the barrier, are still clearly visible. However, it is possible to identify higher order reflections of these pulses which, before reaching the receivers, have hit the lateral walls, creating an even more complicated wave field.

The last two rows of Fig. 2 include snapshots which illustrate the responses calculated at $t = 240.3$ ms. In the absence of any acoustic barrier and lateral walls, the pulses have now traveled away from the grid of receivers (not presented). When a lateral wall is inserted, the additional set of pulses originated from the reflections on this wall is still visible as a propagating set of pulses travelling towards the left (see Fig. 2b; $t = 240.3$ ms). The two sets of reflection pulses, originated when the two lateral walls are inserted, are still visible, but they have already hit the opposite wall and started to propagate in the opposite direction (see Fig. 2c; $t = 240.3$ ms). As time progresses, these pulses are subjected to multiple reflections, and the wavefront gets larger, becoming flatter and remaining trapped between the two lateral walls until the energy dissipates.

When the barrier is inserted between the source and the receivers, the waves first reflected on the building and lateral walls may strike the rigid surface of the barrier, and remain trapped between the barrier and the building. When the 2.0 m tall acoustic barrier is present, the time domain responses reveal the presence of these trapped waves. Fig. 2b and c ($t = 240.3$ ms) illustrate the presence of these waves, which decay very quickly as the distance from the ground becomes greater than the height of the barrier. For a taller barrier (6.0 m), these multiple reflections are even more noticeable, as they are still visible further away from the ground.

4.2. Time responses generated by source 2

Fig. 3 shows the snapshots generated by source 2, located at $x = 25.0$ m, $y = 0.6$ m and $z = 45.0$ m, for the time frames defined previously, when a barrier 6.0 m tall is placed between the source and the building.

At time $t = 90.6$ ms, when the lateral wall is absent, the response recorded at the receivers exhibits the same features recorded when source one is excited. When the lateral wall is placed at $z = 50.0$ m, 5.0 m from the source, the response shows an additional set of pulses generated by the interaction of the waves reflected on the lateral wall, after being diffracted by the barrier. At this time the different pulses are not yet seen as fully separated. The response does not change with the introduction of the second lateral wall at $z = 0.0$ m, since no waves have arrived at this plane.

As time passes, these pulses become better separated and can be easily distinguished. At $t = 120.3$ ms and when the lateral confinement is absent, the direct pulses diffracted on the barrier and those first reflected on the ground are visible as two separate wavefronts. When the lateral wall is placed at $z = 50.0$ m, two additional sets of pulses are identifiable, corresponding to the first reflections of the former

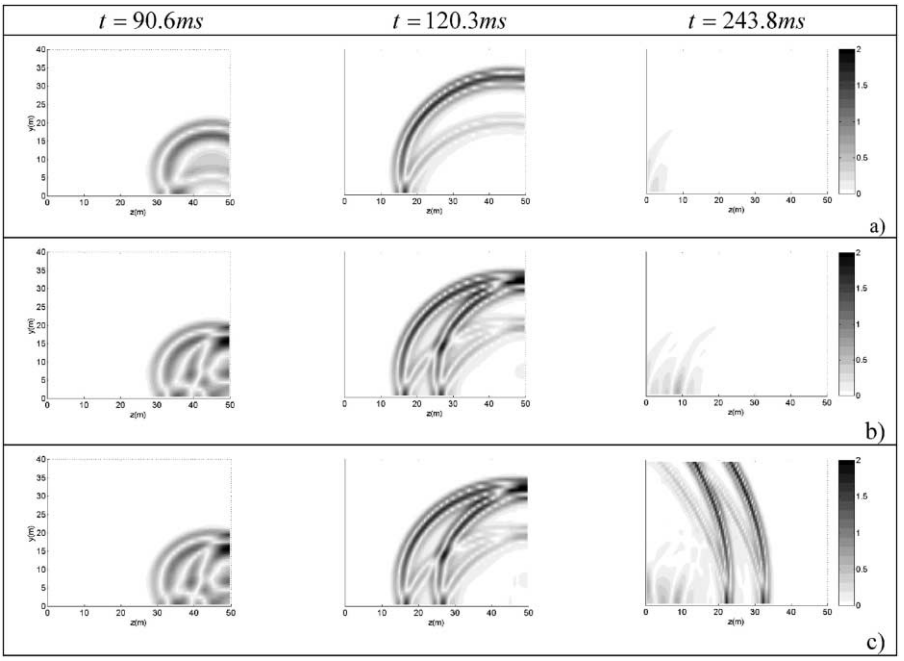

Fig. 3. Time domain responses for the different scenarios when source 2 is excited in the presence of a barrier 6.0 m tall: (a) no lateral confinements; (b) one lateral wall at $z = 50.0$ m; (c) two lateral walls at $z = 0.0$ m and $z = 50.0$ m.

pulses on the surface of the lateral wall. Again, the response remains the same when the second lateral wall is placed at $z = 0.0$ m, since the waves have not yet struck this plane. As time progresses, additional pulses are originated by the waves that become trapped between the acoustic barrier, the building and the lateral walls. These pulses decay very quickly as the distance from the ground increases above the height of the barrier.

At $t = 240.3$ ms and when the lateral confinement is absent, the former pulses have propagated further away from the source, and the remaining pulses recorded at the selected receivers are mainly caused by the presence of these trapped waves. Similar behavior is observed when one lateral confinement is placed at $z = 50.0$ m. When two lateral walls are included, these same trapped pulses are still visible. However, additional trapped pulses are present as the result of the lateral confinement. These pulses will keep travelling back and forward between the lateral walls until all the energy spreads out.

4.3. Evaluation of the pressure level and SPL attenuation

The time domain responses presented before are the basis for calculating the sound pressure level (SPL) over the vertical grid of receivers placed at $x = 0.5$ m. To calculate the SPL in dB, the expression $10\log\left[p^2/\left(2 \times 10^{-5}\right)^2\right]$ is used, where 2×10^{-5} is the reference pressure and p refers to the maximum amplitude of the time

responses calculated for each receiver. The SPL attenuation is calculated as the difference between the SPL obtained in the absence of any acoustic barrier and the SPL calculated in the presence of an acoustic barrier. This procedure is illustrated in Fig. 4. It represents the solution obtained when the lateral walls are absent.

These plots use a gray scale, ranging from white to black as the amplitude increases. When no acoustic barrier is inserted between the source and the building (see Fig. 4a), the pressure field results from the direct incident waves interacting with those reflected by the ground surface and by the building. Thus, the total wavefield represents the sum of acoustic waves, with different phases, which leads to a spatially variable sound pressure level, distinguishable in Fig. 4 as a pattern of differently colored zones.

Fig. 4b shows the sound pressure level, as a pattern of different tones, calculated as described above, when a barrier 6.0 m tall is inserted between the source and the building. Fig. 4c displays its attenuation. The results obtained indicate that the barrier performs less well for receivers placed closer to the ground, owing to the interaction of the direct field diffracted by the barrier with that reflected by the ground surface.

4.4. Barrier SPL attenuation

Fig. 5 presents the SPL attenuation calculated by the procedure described above for the different scenarios when source 1 is excited. Again, the plots in this figure use a gray scale, ranging from white to black as the attenuation increases.

The results obtained for the two barriers in the absence of any lateral confinement (Fig. 5a) confirm the results obtained in previous work by the authors [9], clearly showing that the higher values of attenuation do not occur for receivers in the immediate vicinity of the ground. The results presented in this section and the time domain responses presented above reveal that this behavior is caused by the interaction of pulses caused by the direct diffraction from the edge of the barrier and pulses that are reflected on the ground after being diffracted on the acoustic barrier.

The attenuation provided by the barriers suffers a global decrease when one lateral wall is introduced at $z = 50.0$ m (Fig. 5b). This is particularly evident at specific zones, mainly because of the interaction of pulses reflected by the rigid lateral wall with those directly striking the grid of receivers. It is also possible to note that the

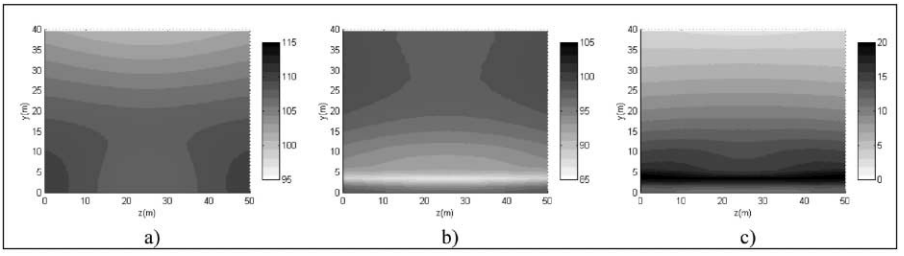

Fig. 4. Calculation of SPL attenuation produced by an acoustic barrier 6.0 m tall: (a) SPL in the absence of the barrier; (b) SPL when the barrier is introduced; (c) SPL attenuation.

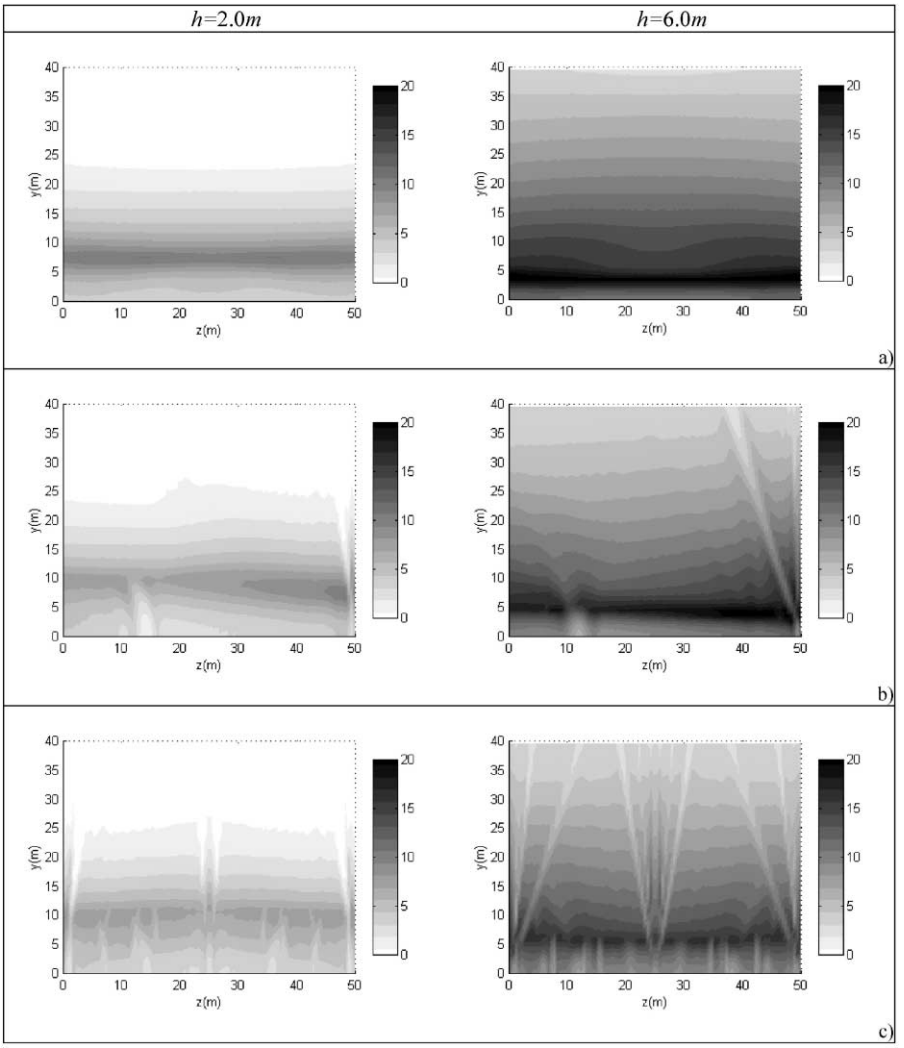

Fig. 5. Sound pressure level attenuation for the different scenarios: (a) no lateral confinements; (b) one lateral wall at $z = 50.0$ m; (c) two lateral walls at $z = 0.0$ m and $z = 50.0$ m.

higher values of attenuation occur for receivers placed closer to the lateral wall, but not in its immediate vicinity. This is the same effect as the one observed for the receivers placed close to the ground surface, caused by the interaction between pulses arriving at the receivers, coming directly from the edge of the barrier, and the pulses that are reflected on the ground after being diffracted on the acoustic barrier. Now, the interacting waves are those coming directly from the edge of the barrier and those pulses reflected on the lateral wall, after being first diffracted on the acoustic barrier. Furthermore, it is possible to observe that the attenuation decreases as the distance from the lateral wall increases. This can be explained by the fact that

as the receivers are further away from the lateral wall, the wavefield reaching those receivers is composed of waves traveling in multiple path directions, creating a diffuse sound field. Analysis of the results also reveals a drop in attenuation, caused by the waves trapped by the barrier and the building and the lateral wall.

When a second lateral wall is introduced ($z = 0.0$ m), the attenuation further decreases, owing to the interaction of the various pulses produced (Fig. 5c). There are well-defined zones where the decrease in attenuation is pronounced. Attenuation behind the barrier, in particular, suffers a pronounced decay for receivers located at

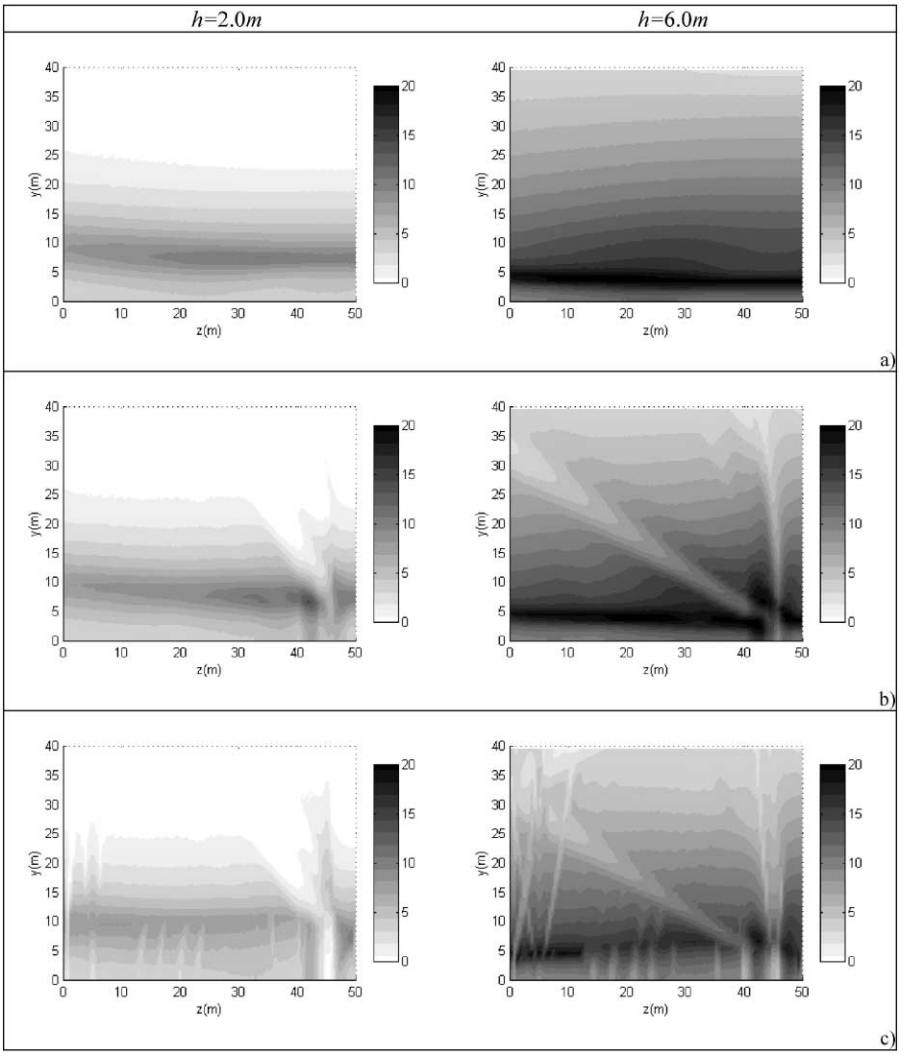

Fig. 6. Sound pressure level attenuation for the different scenarios when the source is at $z = 45.0$ m: (a) no lateral confinements; (b) one lateral wall at $z = 50.0$ m; (c) two lateral walls at $z = 0.0$ m and $z = 50.0$ m.

distances from the ground surface that are less than the height of the barrier. This effect is due to the wavefield produced by the trapped waves within the rectangular box created by the building, the lateral walls and acoustic barrier. Since the source is located along a plane of symmetry, the attenuation results are symmetric.

Fig. 6 shows the SPL attenuation when source 2 is excited. The computed results for the two barriers, in the absence of any lateral confinement (Fig. 6a), exhibit similar wave patterns to the ones described above (see Fig. 5a). As before, the attenuation provided by the acoustic barrier registers a global decrease when one lateral wall is placed at $z = 50.0$ m (Fig. 6b). The interaction between pulses reflected by the rigid lateral wall and those directly striking the grid of receivers, after diffraction at the barrier, is still easily visible. Additionally, the interaction between the pulses reflected by the lateral wall and those hitting the grid of receivers, after being reflected on the ground, generates a pronounced drop in attenuation, which is registered at receivers placed along an inclined line. The SPL attenuation further decreases when a second lateral wall is introduced ($z = 0.0$ m). The same type of scattering phenomena registered when only the first lateral wall is included can also be observed when a second lateral wall is introduced. Besides these interactions, the confined space defined by the two lateral walls creates a set of reflected pulses which travel back and forward between them, leading to additional falls in SPL attenuation. For receivers located at distances from the ground surface that are less than the height of the barrier, the confined space created by the lateral walls, the acoustic barrier and the building façade produces a wavefield, which leads to a further increase of the SPL behind the barrier. This behavior is even more pronounced as the height of the barrier increases. Our results indicate that the acoustic barrier performs better for receivers placed at distances from the ground greater than its height.

5. Conclusions

A 2-1/2D BEM was formulated to study the influence of an acoustic barrier placed between a point sound pressure load and a very tall building. The effect on the attenuation provided by the acoustic barrier by the presence of lateral buildings confining one or both sides of the barrier has been studied.

Time-domain analyses were performed to illustrate the influence of the acoustic barrier on the propagation of a spherical pulse. This analysis confirmed the interaction between pulses diffracted directly at the edge of the barrier and pulses first reflected on the rigid ground, generating an enhanced field in the direct vicinity of the ground. As the lateral walls were introduced to model the presence of lateral buildings, the results were further complicated by the existence of multiple scattered pulses, which interact together, reducing the attenuation provided by the barrier. These interactions were particularly relevant for receivers placed lower down, owing to the presence of a wavefield, generated by the presence of trapped waves between the building, the lateral walls, and the acoustic barrier.

The sound pressure level and the attenuation provided by the acoustic barrier reflected the set of phenomena registered in the time responses. Receivers in the

immediate vicinity of the ground show that the interaction between the direct field, diffracted by the edge of the barrier, and that first reflected on the ground leads to a poorer performance by the barrier. The use of taller barriers ensures that the sound pressure level attenuation increases. Maximum efficiency was found at receivers placed at a certain distance from the ground.

When the lateral walls are introduced, the scattered field increases giving rise to waves propagating in all directions and all interacting together, producing a diffuse wavefield which reduces the performance of the acoustic barrier. This behavior is particularly evident for receivers placed below the height of the barrier.

Although pulses with low excitation frequency were used, higher frequency responses would not alter the main features found by this work. A lower level of energy might be trapped behind the acoustic barrier, which could lead to the barrier performing better. However, the same type of acoustic phenomena would be found, with the same consequences computed in the present work.

It should also be noted that, in practical conditions, with non-uniform surfaces of varying impedance and a broad band continuous source covering higher frequencies, some of the effects found in this work are likely to be much less marked. This would be especially true for the constructive interference found between pulses hitting the receiver after being diffracted by the edge of the barrier, and those that are first reflected on the ground.

References

[1] Muradali A, Fyfe KR. A study of 2D and 3D barrier insertion loss using improved diffraction-based methods. Appl Acoust 1998;53:49–75.
[2] Beranek LL, Vér IL. Noise and vibration control engineering. Wiley Interscience, 1992.
[3] Duhamel D. Efficient calculation of the three-dimensional sound pressure field around a noise barrier. J Sound Vib 1996;197(5):547–71.
[4] Duhamel D, Sergent P. Sound propagation over noise barriers with absorbing ground. J Sound Vib 1998;218(5):799–823.
[5] Morgan PA, Hothersall DC, Chandler-Wilde SN. Influence of shape and absorbing surface—a numerical study of railway barriers. J Sound Vib 1998;217(3):405–17.
[6] Lacerda LA, Wrobel LC, Mansur WJ. A dual boundary element formulation for sound propagation around barriers over an infinite plane. J Sound Vib 1997;202:235–347.
[7] Lacerda LA, Wrobel LC, Power H, Mansur WJ. A novel boundary integral formulation for three-dimensional analysis of thin acoustic barriers over an impedance plane. J Acoust Soc Am 1998;104-2: 671–8.
[8] Jean P, Defrance J, Gabillet Y. The importance of source type on the assessment of noise barriers. J Sound Vib 1999;226(2):201–16.
[9] Godinho L, António J, Tadeu A. 3D sound scattering by rigid barrier in the vicinity of tall buildings. Appl Acoust (to appear).
[10] Godinho L, Tadeu A, Branco F. 3D acoustic scattering from an irregular fluid waveguide via de BEM. Eng An Bound El (to appear).
[11] Tadeu A, Pereira A, Godinho L. Three dimensional wave scattering by rigid circular pipelines in an acoustic waveguide. J Comp Mod Eng Sci 2001;2(1):49–61.
[12] Kausel E. Forced vibrations of circular foundations in layered media (MIT Research Report 70-3). Cambridge, USA: Department of Civil Engineering, MIT, 1974.